A genomic view of coral-associated *Prosthecochloris* and a companion sulfate-reducing bacterium

Yu-Hsiang Chen[1,2,3]*, Shan-Hua Yang[4]*, Kshitij Tandon[1,2,5], Chih-Ying Lu[1], Hsing-Ju Chen[1], Chao-Jen Shih[6], Sen-Lin Tang[1,2#]

[1]Biodiversity Research Center, Academia Sinica, Taipei 115, Taiwan

[2]Bioinformatics Program, Institute of Information Science, Taiwan International Graduate Program, Academia Sinica, Taipei 115, Taiwan

[3]Graduate Institute of Biomedical Electronics and Bioinformatics, National Taiwan University, Taipei 10617, Taiwan

[4]Institute of Fisheries Science, National Taiwan University, Taipei 10617, Taiwan

[5]Institute of Molecular and Cellular Biology, National Tsing Hua University, Hsinchu 300, Taiwan

[6]Bioresource Collection and Research Center, Food Industry Research and Development Institute, Hsinchu 30062, Taiwan

*These authors contributed equally to this work.

Corresponding author

Corresponding author Email: sltang@gate.sinica.edu.tw

Abstract

Endolithic microbial symbionts in the coral skeleton may play a pivotal role in maintaining coral health. However, compared to aerobic microorganisms, research on the roles of endolithic anaerobic microorganisms and microbe-microbe interactions in the coral skeleton are still in their infancy. In our previous study, we showed that a group of coral-associated *Prosthecochloris* (CAP), a genus of anaerobic green sulfur bacteria, was dominant in the skeleton of the coral *Isopora palifera*. Though CAP is diverse, the 16S rRNA phylogeny presents it as a distinct clade separate from other free-living *Prosthecochloris*. In this study, we build on previous research and further characterize the genomic and metabolic traits of CAP by recovering two new near-complete CAP genomes—*Candidatus* Prosthecochloris isoporaea and *Candidatus* Prosthecochloris sp. N1—from coral *Isopora palifera* endolithic cultures. Genomic analysis revealed that these two CAP genomes have high genomic similarities compared with other *Prosthecochloris* and harbor several CAP-unique genes. Interestingly, different CAP species harbor various pigment synthesis and sulfur metabolism genes, indicating that individual CAPs can adapt to a diversity of coral microenvironments. A novel near-complete SRB genome—*Candidatus* Halodesulfovibrio lyudaonia—was also recovered from the same culture. The fact that CAP and various sulfate-reducing bacteria (SRB) co-exist in coral endolithic

cultures and coral skeleton highlights the importance of SRB in the coral endolithic community. Based on functional genomic analysis of *Ca.* P. sp. N1 and *Ca*. H. lyudaonia, we also propose a syntrophic relationship between the SRB and CAP in the coral skeleton.

Importance

Little is known about the ecological roles of endolithic microbes in the coral skeleton; one potential role is as a nutrient source for their coral hosts. Here, we identified a close ecological relationship between CAP and SRB. Recovering novel near-complete CAP and SRB genomes from endolithic cultures in this study enabled us to understand the genomic and metabolic features of anaerobic endolithic bacteria in coral skeletons. These results demonstrate that CAP members with similar functions in carbon, sulfur, and nitrogen metabolisms harbor different light-harvesting components, suggesting that CAP in the skeleton adapts to niches with different light intensities. Our study highlights the potential ecological roles of CAP and SRB in coral skeletons and paves the way for future investigations into how coral endolithic communities will respond to environmental changes.

Introduction

Microbial symbionts in reef-building corals, which support a variety of marine life, reside in the mucus, tissue, and skeleton of diverse corals, influencing health of its host coral (1, 2). Microbial symbionts comprise bacteria, archaea, algae, fungi, and viruses, and their composition is influenced by their host corals' genetic factors and dynamic environmental conditions (3). They can help corals prevent or mitigate diseases and benefit corals by involving them in carbon, nitrogen, and sulfur cycles (4). For example, coral dominant dinoflagellate *Symbiodinium* can fix carbon dioxide and provide corals with organic compounds (5). On the other hand, *Cyanobacteria* can fix nitrogen and provide the coral *Montastraea cavernosa* with a nitrogen source (6).

Compared to aerobic microorganisms, the role of anaerobic microorganisms in coral is not well understood. Previous studies found green sulfur bacteria (GSB) in a wide range of corals, including *Porites lutea*, *Platygyra carnosa*, *Montastraea faveolata* and *Montipora venosa* (7-10). In addition, our previous study found that *Prosthecochloris*, a GSB genus, was dominant in skeletons of the coral *Isopora palifera*, forming a distinct green color region beneath the coral tissue (11), although the algae *Osterobium* were previously thought to be the main microbial contributor to coral green layers (11-13). Moreover, nutrients generated from microorganisms in the coral skeleton were shown to

be potential alternative sources of energy and nutrients (14, 15). Therefore, the *Prosthecochloris* dominant in green layers may also be associated with stony coral health.

Most GSB are obligate anaerobic photoautotrophic bacteria that use the reverse tricarboxylic acid (rTCA) cycle to fix carbon dioxide (16). During photosynthesis, the majority of them utilize reduced sulfur compounds as electron donors, while some—including *Chlorobium ferrooxidans* and *C. phaeoferrooxidans*—use ferrous iron (17-19). Furthermore, some GSB are capable of obtaining reduced sulfur compounds through a syntrophic interaction with sulfur-reducing bacteria (SRB), such as *Desulfuromonas acetoxidans* (20). On the other hand, many GSB can fix nitrogen gas, which they use for growth (16). GSB are found in various anoxic environments—including freshwater, hot springs, and seawater—and some of them are adapted to light-limited environments (16). Among GSB, *Prosthecochloris* is mainly present in marine environments and has the ability to tolerate high salinity (16).

Though *Prosthecochloris* and most other GSB have been isolated as free-living bacteria (16), our previous study used amplicon and whole-metagenome analyses and found that *Prosthecochloris* is dominant in green layers of coral *Isopora palifera* skeletons, suggesting that the bacteria can interact with eukaryotic hosts and various bacteria (11, 13). Through a phylogenetic analysis of the 16S rRNA gene, we found that, although

Prosthecochloris from coral were diverse, they could be classified into a monophyletic clade separate from other free-living *Prosthecochloris*. Hence, we proposed a group of coral-associated *Prosthecochloris* (CAP) (11). Furthermore, based on a gene-centric metagenome analysis, we proposed that CAP can fix nitrogen and nutrient cycling occurs in the coral skeleton.

The role of endolithic microbiomes in the coral reef system has been overlooked (21). To provide detailed insights into the ecological roles of CAP and microbe-microbe interactions in the coral skeleton, high-quality genomes of endolithic microbes are needed. The genome for the CAP *Candidatus* Prosthecochloris A305, which we identified by metagenome-binning, is only 79% complete. Other metagenomic bins identified were highly contaminated with other species. These results hindered our understanding of the metabolic features of CAP and illuminated syntrophic relationships between CAP and other microorganisms in the coral skeleton. Using an anaerobic culture approach, three endolithic cultures dominated by CAP were successfully obtained. The cultures, containing purer and more simplified communities and sufficient genomic DNA, enabled us to obtain the high-quality genomes of CAP and other companion bacteria using whole-metagenome sequencing approach. In this study, we recovered two near-complete CAP genomes from the metagenomes of the coral endolithic cultures. These new genomes allowed us to

compare functional genomic and phylogenetic features in CAP and to elucidate its diversity. Moreover, we also identified a novel, predominant sulfate-reducing bacteria (SRB) genome from the same cultures. Based on functional genomic analysis in these genomes, we propose a syntrophic relationship between CAP and SRB in the coral skeleton.

Results

High-quality bins recovered from coral endolithic cultures

Reads from coral endolithic cultures (N1, N2, and N3) were individually *de novo* assembled and binned, yielding 5, 5, and 4 bins, respectively (Table 1). Bins from cultures had similar taxonomic profiles, dominated by *Prosthecochloris*-related bins in N2 and N3 and *Ilyobacter*-related bins in N1 (Table S1). On the other hand, *Halodesulfovibrio*-related bins were the most abundance sulfate-reducing bacterial bins in the three coral endolithic cultures. Other genera represented in bins were *Marinifilum, Pseudovibrio,* and *Desulfuromonas*, which were present in two of the three cultures. Among the total 14 bins identified, nine were high-quality (>90% complete and <5% contamination). The *Prosthecochloris*-related bins had particularly high quality (>98.8% complete) and low contamination (<1.5%); *Halodesulfovibrio*-related bins in N3 was also near-complete (99.41%) with very low contamination (0.26%) (Table 1). Both *Prosthecochloris*- and

Halodesulfovibrio-related bins lacked strain heterogeneity.

Novel near-complete coral-associated *Prosthecochloris* (CAP) draft genomes from coral endolithic cultures

The results of the GTDB-Tk taxonomy assignment showed that all bins were closest to *Prosthecochloris marina* V1. Interestingly, *Prosthecochloris*-related bins in N2 and N3 shared only 90% Average Nucleotide Identity (ANI) with *Prosthecochloris* marina V1 (Fig. S1), which is below the 95% ANI cutoff, a frequently used standard for species delineation (22). On the other hand, the ANI between *Prosthecochloris*-related bins in N2 and N3 was 99.9%, suggesting that the bins were identical, and these bins were named *Candidatus* Prosthecochloris isoporaea. The draft genome of *Ca*. P. isoporaea was 2.6 Mb with 47.4% GC, which is within the range of *Prosthecochloris* genomes (2.4 - 2.7 Mb with 47.0 - 56.0% GC). The N50 of the draft genomes in N2 and N3 were 65 and 92 kbp, respectively. The contig numbers were 51 and 49, and the longest contig was 309 and 225 kbp, respectively. The longest contig of the *Ca*. P isoporaea genome in N2 was larger, so this genome was used as the representative genome for all downstream analysis.

The ANI between the *Prosthecochloris*-related bin in N1 and *Prosthecochloris marina* V1 was 99%, suggesting that these genomes belong to the same species. The bin was named

145 *Candidatus* Prosthecochloris sp. N1. Its genome size was 2.7 Mb, with 23 contigs and a
146 47.0% GC ratio, which is consistent with the genome of *Prosthecochloris* marina V1 (23).
147 The ANI between these newly identified genomes and other *Chlorobiaceae* members
148 was also determined (Fig. S1). *Ca*. P. isoporaea and *Ca*. P. sp. N1 shared the highest ANI
149 value with *Candidatus* Prosthecochloris sp. A305 (~79%) and *Candidatus* Prosthecochloris
150 korallensis (~80%), which were both previously identified from the coral metagenomes
151 and defined as part of the coral-associated *Prosthecochloris* (CAP) group (11). Furthermore,
152 the genomes of *Candidatus* Prosthecochloris sp. A305 and *Candidatus* P. korallensis were
153 most similar (82% ANI) (Fig. S1). These results indicated high genomic similarities
154 between the members of CAP. The other *Chlorobiaceae* closest to CAP were
155 *Prosthecochloris* sp. GSB1 and *Chlorobium phaeobacteroides* BS1, later annotated as
156 *Prosthecochloris phaeobacteroides* BS1 (7).
157
158 **Phylogenetic tree of CAP and other green sulfur bacteria**
159 To determine the phylogenetic relationship between CAP and other members of
160 *Chlorobiaceae*, 16S rRNA gene sequences of CAP-related genomes and other
161 *Chlorobiaceae* were used to reconstruct phylogenetic trees (Fig. 1A). The analysis also
162 included *Prosthecochloris*-related Operational Taxonomic Units (OTU) (at species-like

163 level), which we identified from the green layer of coral *Isopora palifera* (11); bin-3, which
164 was recovered from metagenomes in the green layer of *Isopora palifera* (11); and one
165 uncultured clone isolated from the coral *Montastraea faveolata* (24). All CAP members
166 were grouped into the same clade, and the clade closest to it contained other free-living
167 *Prosthecochloris*. The tree based on FMO, a unique photosynthetic-related protein in
168 *Chlorobiaceae*, also classified the CAP members into the same clade, with the addition of
169 *Chlorobium phaeobacteroides* BS1 and *Prosthecochloris* sp. GSB1 (Fig. 1B). In addition,
170 to more confidently establish the evolutionary relationships, we also used concatenated
171 protein sequence alignments of common single-copy genes in these genomes to construct
172 the tree. The results demonstrated that the CAP forms a unique clade, irrespective of the
173 sequences used (Fig. 1C). These congruent results indicate that CAP have a unique
174 evolutionary origin.
175
176 **Pan-genome analysis of *Prosthecochloris***
177 Pan-genome analysis was conducted to understand the core-accessory relationships in
178 the genus *Prosthecochloris*. The plot of pan-genome size along the number of genomes
179 indicated that the pan-genome is open (Fig. S2A). The *Prosthecochloris* genomes share
180 442 core genes (Fig. S2B). The number of genes absent only in *Candidatus*

Prosthecochloris sp. A305 is 122, which may indicate that the draft genome is incomplete. The COG and KEGG classification of the core, accessory, and unique proteins revealed that the translation, energy production, and amino acid metabolism categories had higher proportions of core proteins than accessory or unique proteins (Fig. S3A and B). On the other hand, the drug resistance, secondary metabolite biosynthesis, DNA replication, and membrane transport categories had higher proportions of accessory and unique proteins (Fig. S3A and B). The phylogeny of concatenated alignment of core protein sequences grouped CAP members in the same clade (Fig. S4), with *P.* sp GSB1 and *C. phaeobacteroides* BS1 as closest relatives. The CAP clade contained 213 clade-specific accessory genes. In addition, we also found 80 genes present in all CAP genomes, except that of A305. The 213 accessory genes and these 80 genes were searched using BLASTn against the NCBI RefSeq database. The results showed that, although most genes had orthologue genes in other *Chlorobiaceae* members, some were unique to CAP members (Table S2). It is noteworthy that the putative gene sources of many BLASTn top hits were from sulfate-reducing bacteria. Moreover, the *dN/dS* ratio of these genes were < 0.3, indicating that the changes in amino acid sequences in these gene coding sequences were deleterious.

Metabolic characteristics of CAP

The KEGG annotation by BlastKoala revealed that all the CAP members have nitrogen fixation genes—except for *Ca*. P. A305—and lack the genes for dissimilatory nitrate reduction pathway and denitrification—except for *Ca.* P. korallensis, which contains genes responsible for converting nitrite to ammonia (Table S3). For the carbon metabolism pathway, all the CAP members have a complete gene repertoire for the rTCA cycle—except for *Ca*. P. A305, which lacks the *idh* gene. On the other hand, the gene encoding phosphoenolpyruvate carboxylase (*ppc*) is only present in *Ca*. P. A305 and *Ca*. P. korallensis and the carbon monoxide dehydrogenase coding gene (*cooF* or *cooS*) is only present in *Ca*. P. korallensis and *Ca*. P. sp. N1.

For the sulfur metabolism pathways, *sqr* and *fccAB*—encoding sulfide-quinone reductase and sulfide dehydrogenase, respectively—were identified in all CAP members. Complete dissimilatory sulfate reduction (DSR) and thiosulfate reductase pathway encoding genes were identified in all members of CAP except *Ca*. P. A305. In addition, the genomes of *Ca*. P. isoporaea and *Ca*. P. sp. N1 also contained all genes in the assimilatory sulfate reduction and thiosulfate-oxidizing Sox enzyme systems, except for the *soxCD* genes.

Distinct colors of the N1 (green) and N2 (brown) cultures led us to hypothesize that

CAP can harbor different bacteriochlorophylls (BChl), as a previous study showed that brown-color GSB have BChl *e* (19). The KEGG results showed that all CAP members have the genes to synthesize BChl *a*, BChl *b*, and BChl *d* from chlorophyllide *a* (Table S3), but the *bciD* gene—encoding the enzyme that converts bacteriochlorophyllide *c* to bacteriochlorophyllide *e*—is only present in *Ca*. P. isoporaea. Moreover, our previous analysis of the absorption spectrum revealed the presence of BChl *e* in the N2 culture only (11). These results implied that the presence of *bciD* gene might enable *Ca*. P. isoporaea to synthesize BChl *e*, suggesting that the differences in genes responsible for pigment synthesis could be responsible for the color difference in the N1 and N2 cultures.

The transporter systems in CAP were also identified by BlastKoala (Table S3). The results demonstrate that CAP have the ABC transporter systems for transporting molybdate, nucleoside, phospholipid, phosphate, lipoprotein, lipopolysaccharide, and cobalt. In addition, sulfate, ammonium, and drug/metabolite transporters were also identified by annotation in transportDB 2.0 (DATA SET S1).

Recovered novel sulfate-reducing bacteria genome in coral endolithic cultures

Our binning results showed that the *Halodesulfovibrio*-related bin was present in all coral endolithic cultures, and the bin in N3 is nearly complete (99.41%) and has very low

235 contamination (0.26%) (Table 1). The closest available genome to this bin is
236 *Halodesulfovibrio marinisediminis*, with an ANI of 84.1%, suggesting that the bin belongs
237 to a novel species. Hence, the bin was renamed as *Candidatus* Halodesulfovibrio lyudaonia.
238 The total length of the draft genome is 3.7 Mb, comprising 81 contigs with a 44.9% GC
239 ratio.

240 The ANI between the genomes of existing *Halodesulfovibrio* species and *Ca*. H.
241 lyudaonia was 83 to 84%. As *Halodesulfovibrio* originally belonged to the *Desulfovibrio*
242 genus, the ANI between *Desulfovibrio* and *Ca*. H. lyudaonia was also determined, which
243 demonstrated that *Ca*. H. lyudaonia and some *Desulfovibrio* species share >70% ANI. The
244 phylogenetic analysis of 16S rRNA and whole-genome similarity revealed that the
245 *Halodesulfovibrio* could be separated from *Desulfovibrio* as a monophyletic clade (Fig.
246 S5A and B). Besides, the 16S rRNA analysis also showed that *Ca*. H. lyudaonia and
247 *Halodesulfovibrio*-related 16S rRNA in the N1 culture could be classified into a clade with
248 *H. marinisediminis* and *H. spirochaetisodalis* (Fig. S5A).

249 The genomic analysis within sulfur metabolism revealed that all the existing
250 *Halodesulfovibrio* and *Ca.* H. lyudaonia have dissimilatory sulfate reduction and *sqr* genes
251 (Table S4). For the nitrogen metabolism, the nitrogen-fixation genes were only identified
252 in *H. aestuarii,* and denitrification and nitrate reduction-related genes were absent in all

genomes (Table S4). For carbon metabolism, genes participating in glycolysis and ethanol fermentation were present in all *Halodesulfovibrio*. Moreover, all genomes contained multiple genes encoding formate dehydrogenase, which helps convert formate to CO_2.

The transporter gene analysis revealed the existence of molybdate, nucleoside, phospholipid, phosphate lipopolysaccharide, cobalt, phosphonate, glutamine, branched-amino, zinc, and tungstate transporter genes in *Halodesulfovibrio* (Table S4). Furthermore, the general L-amino acid and sulfate transporter genes were also identified in the *Ca*. H. lyudaonia. Different *Halodesulfovibrio* species contained various secretion systems. *Halodesulfovibrio* have genes responsible for the Type II secretion system, twin-arginine translocation pathway, and general secretory pathway (Table S4). Apart from these systems, the *Ca*. H. lyudaonia also had genes involved in the Types III and VI secretion systems.

Discussion

In this study, we used genomic and functional genomics analyses to characterize coral-associated *Prosthecochloris* (CAP) and a companion sulfate-reducing bacterium. Two near-complete and high-quality CAP draft genomes were recovered from coral endolithic cultures, including one novel species. The genomic and functional analysis of existing CAP members revealed a functional diversity between the members, in spite of their

phylogenetic closeness and genome similarities. Along with CAP, sulfate-reducing bacteria (SRB) were also common in endolithic cultures, indicating a potential symbiotic relationship between the groups. Hence, a near-complete draft genome of a novel species in *Halodesulfovibrio*—a common SRB genus in coral endolithic cultures—was also recovered and functional genomics analysis performed. Based on the metabolic features of the CAP and SRB genomes, a putative syntrophic interaction between the *Halodesulfovibrio* and CAP was proposed.

CAP formed a monophyletic clade and shared several CAP-specific genes

Prosthecochloris is the only green sulfur bacterial genus found in green layers of coral skeleton to date. Furthermore, CAP can be phylogenetically separated from other free-living *Prosthecochloris*, suggesting that they share certain common features enabling them to live in diverse microenvironments of the coral skeleton. Interestingly, pan-genome analysis identified several genes that were unique to CAP. The similarity search results revealed that most of these genes were from SRB, suggesting a close ecological relationship between SRB and CAP members and maybe even a history of horizontal gene transfer. These CAP-unique genes had a low ratio of nonsynonymous to synonymous substitutions ($dn/ds<1$), indicating that these genes underwent purifying selection;

289 therefore, mean the changes in the overall amino acid sequences of these genes would
290 decrease bacteria fitness.

291 We propose two hypotheses about the ancestor of CAP. First, it acquired these genes
292 while living in coral skeletons, and these genes were selected for. Second, it lived in other
293 microbial communities and, after acquiring the above mentioned genes, gained fitness to
294 live in coral environments. For example, among the CAP-specific genes, we found that
295 there is a tripartite ATP-independent periplasmic transporter (TRAP transporter) gene
296 cassette that includes permease and a substrate-binding subunit. TRAP is a protein family
297 involved the bidirectional transport of a wide range of organic acids (25). CAP could
298 potentially use this transport system to acquire important nutrients from the specific coral-
299 built environment.

300

301 **CAP possess different photosynthetic machinery**

302 Green sulfur bacteria (GSB) are obligate anaerobic photoautotrophs that use light as
303 an energy source to grow (19). Photosynthesis occurs in self-assembly light-harvesting
304 complexes called chlorosomes, which comprise different types of bacteriochlorophyll
305 (BChl) pigments (19). Though all GSB have BChl in their reaction centers, different
306 members have different antenna pigments, resulting in different colors (16). The major

307 BChls in GSB, including BChl *c*, *d*, or *e*, have different absorption peaks. Green-colored
308 GSB have BChl *c* or *d,* and brown-colored GSB contain BChl *e* in the chlorosome (16).
309 The brown-colored GSB were shown to be well adapted to light-limited environments,
310 such as deeper waters (19). Moreover, a previous study revealed that light conditions in a
311 lake may determine which color of GSB will is the dominant group (16, 26).

312 The coral endolithic cultures N1 and N2, dominated by CAP, were green- and brown-
313 colored, respectively. Our previous study confirmed the presence of BChl *c* and lack of
314 BChl *e* peak in the N1 culture, from which *Candidatus* P. sp. N1 was recovered (11). On
315 the other hand, the BChl *e* was present in the N2 culture, from which *Candidatus* P.
316 isoporaea was identified. The functional genomics analysis in this study suggests that the
317 lack of the *bciD* gene, which participates in BChl *e* biosynthesis, may account for the
318 absence of BChl *e* in *Ca.* P. sp. N1, leading to the green coloration (27). This result suggests
319 that CAP members may possess different photosynthetic machinery, which can help which
320 species is dominant under different light conditions in coral skeleton microenvironments.

321 Multiple factors contribute to the variation in light availability of a skeleton
322 microenvironment, including individual differences in skeleton pore size and skeleton
323 structures owing to genetic differences or dynamic environmental factors (28). Light
324 availability also varies at the different depths of the coral tissue (29). Hence, we

hypothesize that the individual difference in skeleton structures and the depth of microhabitat in coral skeleton will influence the distribution of different CAP species. For instance, deeper sections of the skeleton with less light could be dominated by brown-colored CAP, while the regions closer to the surface of coral tissue may be dominated by green-colored CAP (Fig. 2). Confirming this hypothesis requires further investigating pigment contents by determining absorbance spectra in the different sections of a single coral skeleton to establish whether there is any correlation between the distribution of the two specific groups and the depth of the skeleton region.

Sulfur metabolism in CAP

Most GSB species obtain electrons by oxidizing sulfide, sulfur, and thiosulfate for carbon fixation (30, 31). Among oxidative sulfur metabolism pathways, the Sox enzyme system—by which bacteria oxidize thiosulfate—is common. However, using thiosulfate as an electron donor and Sox gene clusters are only found in some GSB (32). In addition, GSB do not have the SoxCD complex, a part of the Sox system that is integral for oxidizing thiosulfate to sulfate in many other bacteria; instead, the function of SoxCD is replaced by the dissimilatory sulfate reduction (DSR) system in GSB (16, 33, 34). Moreover, many GSB use the DSR system to oxidize polysulfide to sulfite. Thus, in GSB, the DSR system

343 is required to complete the oxidation of sulfur compounds. In CAP, *Ca*. P. isoporaea and
344 *Ca.* P. sp. N1, identified from the coral skeleton, contain all genes involved in DSR and the
345 Sox system—except for *soxCD*—indicating that GSB can obtain electrons by oxidizing
346 sulfide, sulfite, and thiosulfate, which is similar to the way that *Chl*. *tepidum* operates (35).
347 However, *Ca*. P. korallensis, identified from homogenized corals, only have the DSR
348 system. With the DSR system, GSB are better able to utilize reduced sulfur compounds,
349 which might confer additional advantages in sulfide- and energy-limited conditions.
350 However, *Ca*. P. korallensis lacks the Sox system. This may due to the differences in the
351 availability of sulfur compounds inside corals, which contribute to the diverse sulfur
352 metabolism in CAP or the incompleteness of *Ca*. P. korallensis genome.

353 In some anaerobic systems, the syntrophic interaction between GSB and sulfur-
354 reducing bacteria (SRB) occurs because sulfate produced by GSB is used as an electron
355 acceptor in SRB, and biogenic sulfide produced by SRB is used as an electron donor in
356 GSB (20). The binning results and our previous 16S rRNA gene-based analysis in
357 endolithic cultures revealed the presence of potential SRB including *Halodesulfovibrio*,
358 *Desulfovibrio*, and *Desulfuromonas*. These bacteria are common in the skeleton of *Isopora*
359 *palifera* (11). In the three endolithic cultures, the SRB was predominant in metagenomic
360 sequencing, suggesting that it 1) is the main group providing reduced sulfur compounds as

electron donors for CAP in cultures and 2) plays the synergetic role in the endolithic community in coral skeletons.

A novel sulfate-reducing bacterium genome identified from coral endolithic cultures

Our metagenome analyses demonstrated the relationship between CAP and SRB. The most abundant SRB in our coral endolithic cultures is *Halodesulfovibrio*, which is present in all cultures and also in green layers. Here, we recovered a high-quality near-complete draft genome of a novel species *Candidatus* Halodesulfovibrio lyudaonia. *Halodesulfovibrio* was classified as a novel genus separated from *Desulfovibrio* according to the differences in genome, phylogeny, and phenotype in 2017 (36-38). There are currently only four available species and genomes, which were all identified from marine habitats, including sediment and oxygen minimum zone water columns. Ours is the first study to find that *Halodesulfovibrio* might have a relationship with its eukaryotic host and may have syntrophic relationship with other bacteria.

Previous studies revealed that *Halodesulfovibrio* can use sulfate or sulfite as electron acceptors (38). The presence of all genes involved in the DSR system indicates that these bacteria use this pathway to reduce sulfur compounds (Table S4). In addition, some SRB can also fix nitrogen, such as *Firmicutes* and *Deltaproteobacteria* (39). In our analysis,

379 nitrogen fixation genes were absent in all *Halodesulfovibrio* except *H. aestuarii* (Table S4).
380 However, we also found that bacteria containing the gene encoding L-amino acid and
381 ammonia transporters can be used to obtain organic nitrogen.
382
383 **Putative syntrophic interaction between diverse CAP and *Halodesulfovibrio***
384 Previously, we proposed a general syntrophic interaction based on gene-centric
385 approach with metagenomes of coral skeleton (11). Here, using several high-quality and
386 near-complete draft genomes from endolithic cultures, we identified CAP and SRB species
387 that participate in this syntrophic interaction. Moreover, the high-quality draft genomes
388 also allowed us to characterize communities and interactions in a more accurate and
389 detailed manner. The recovered genomes highlight the diversity in CAP and the complex
390 interactions in the community (Fig. 2).
391 Brown-colored CAP can adapt to low-light microenvironments, and therefore may
392 dominate deeper sections of the skeleton, while green-colored CAP may dominate the
393 sections closer to the coral tissue, which are exposed to relatively higher light intensity. On
394 the other hand, the presence of *Halodesulfovibrio* in all endolithic cultures—along with
395 both brown- and green-colored CAP—suggests that *Halodesulfovibrio* may be distributed
396 across different sections and interact with both colors of CAP. We suggest that both CAP

397 species occupy their niches via diversified pigment compositions, and both interact in a
398 syntrophic manner with *Halodesulfovibrio.*

399 During photosynthesis, these CAP obtain CO_2 released by *Halodesulfovibrio* and
400 other heterotrophs. To fix carbon through the rTCA cycle, CAP obtains sulfide from
401 *Halodesulfovibrio* as an electron donor, while the *Halodesulfovibrio* obtain oxidized sulfur
402 compounds released from CAP and reduce them using electrons from the conversion of
403 formate to CO_2. Therefore, CAP and *Halodesulfovibrio* provide each other with sulfur
404 resources in the coral skeleton.

405 Being the most dominant nitrogen fixers, CAP fixes dinitrogen into ammonium, which
406 can be bi-directionally diffused across the cell membrane into the microenvironment by the
407 ammonium transporter. Although genes involved in nitrogen fixation are absent in
408 *Halodesulfovibrio*, they can take up ammonium through an ammonium transporter, which
409 might serve as a potential nitrogen source. Hence, we suggest that CAP plays an essential
410 role in nitrogen fixation in the community.

411

412

413 ## Conclusion

414 Though the skeleton microbiome may contain nutritional sources and facilitate the

415 recovery of unhealthy coral (15), its importance in the coral skeleton has been overlooked,
416 and the interactions inside the community are poorly studied due to methodological
417 limitations (21). Here, our genomic analysis of endolithic cultures helps us better
418 characterize the community and investigate the interaction between coral and the endolithic
419 microbiome.

420 Endolithic cultures provide several near-complete and precise genomes to study
421 endolithic communities. Genomic analysis revealed that members of CAP share a common
422 origin and contain several CAP-specific genes, indicating that certain differences exist
423 between CAP and other free-living *Prosthecochloris*. These differences imply that coral
424 and CAP have a symbiotic relationship, but future investigations into metabolic exchanges
425 between CAP and the coral host are needed to confirm this. On the other hand, functional
426 genomic analysis revealed the diversity of pigments synthesized in CAP, suggesting that 1)
427 individual members of CAP adapt to different microenvironments in the skeleton and 2)
428 there is spatial heterogeneity in the microbiome. Along with CAP, the predominance of
429 *Halodesulfovibrio* indicates that it is ecologically important in skeleton microbiome
430 communities. Based on their metabolic features, we characterize the carbon, sulfur,
431 nitrogen cycling between *Halodesulfovibrio* and CAP, specifying the metabolic
432 relationships among endolithic microbes in corals.

Method

Sample collection and anaerobic endolithic culturing

Three *Isopora palifera* colonies were collected from the ocean near Gonguuan (22°40' N 121°27' E) in Lyudao, Taiwan (also known as Green Island) on October 16, 2017. These colonies were placed in an anaerobic jar with an anaerobic pack immediately after sampling. Green layers from each colony were collected as described in our previous studies (11, 13). The anaerobic condition was maintained throughout the collection process. Bacteria in the green layers were enriched in the basal medium for *Prosthecochloris*, which consisted of 0.5 g/L KH_2PO_4, 5.3 g/L NaCl, 0.5 g/L $MgSO_4$-$7H_2O$, 0.7 g/L NH_4Cl, 0.33 g/L KCl, 21 g/L Na_2SO_4, 4.0 g/L $MgCl_2$-$6H_2O$, 10 g/L $NaHCO_3$, 0.07 g/L $CaCl_2$-$2H_2O$, and 0.005 g/L Resazurin, and supplemented with glucose (0.05%) as an additional carbon source (11, 40). The entire culturing process was performed under dim light (45.5 ± 31.5 lums/ft^2) conditions.

DNA extraction and whole-genome shotgun sequencing

Bacterial cells in the culture medium were centrifuged at 7,000 x *g* for 10 min at 20°C to obtain cell pellets. Total genomic DNA from the pellet was then extracted using the UltraClean Microbial DNA Isolation Kit (MioBio, Solana Beach, CA, USA) according to

451 the manufacturer's protocol and DNA concentration was determined by Nanodrop and
452 Qubit. The DNA samples were sent to Yourgene Bioscience (Taipei, Taiwan) for library
453 preparation and DNA sequencing by the Illumina MiSeq system (USA) with 2 x 300 cycles.
454
455 **Metagenome assembly and binning**
456 Reads obtained from Illumina MiSeq were quality checked by FastQC (41). Quality
457 trimming and removal of Illumina adaptors were performed by Trimmomatic v0.39 with
458 following parameters: ILLUMINACLIP:TruSeq3-PE-2.fa:2:30:10:3: TRUE
459 LEADING:10 TRAILING:10 SLIDINGWINDOW:5:15 MINLEN:50 CROP:300 (42).
460 Leading and trailing bases with Phred quality score <15 were trimmed using a 5-base wide
461 sliding window. Only reads with >50 bases were retained. The processed reads from three
462 cultures were *de novo* assembled individually using megahit with k-mer sizes of 21, 31, 41,
463 51, 61, 71, 81, 91, and 99 (43) without scaffolding. Automated binning was performed
464 using MetaBAT v0.32.5 with default settings, which reconstructed genomes from
465 assembled metagenomic contigs based on probabilistic distances of genome abundance and
466 tetranucleotide frequency (44).
467
468 **Quality assessment, taxonomic inference, and relative proportion of MAGs**

469 The quality of each metagenome-assembled genome (MAG) was accessed by
470 CheckM v1.0.13, which uses lineage-specific marker genes to estimate completeness and
471 contamination (45). The taxonomy of each MAG was automatically assigned by GTDB-
472 Tk v0.3.2 based on the placement of the genome in the reference tree, Average Nucleotide
473 Identity (ANI) values, and relative evolutionary divergence (RED) values (46). To estimate
474 the relative proportion of MAGs in each culture, reads were first mapped to assembled
475 contigs using Bowtie2 v2.3.5 (47) with default settings. Mapped reads results were then
476 used to obtain coverage for each contig and the relative proportion of each MAG with the
477 'coverage' and 'profile' command in CheckM, respectively.
478
479 **Genome annotation**
480 The genome of coral-associated *Prosthecochloris* (CAP) and *Candidatus*
481 Halodesulfovibrio lyudaonia were annotated using Prokka v1.13.7 with the 'usegenus' and
482 'rfam' options (48). The genomes were also annotated with KEGG functional orthologs (K
483 numbers) by searching the putative protein sequences from Prokka against the KEGG
484 database using BlastKoala (49). The K number annotation results were then used to
485 reconstruct the transporter systems and metabolic pathways using KEGG mapper (50).
486 Additionally, the transporter proteins were identified by searching for the putative protein

487 sequences against TransportDB 2.0 (August 2019) using BLASTp (51).

488

489 **Recruitment of contigs with 16S rRNA gene sequences**

490 The contigs with 16S rRNA gene sequences were originally not binned into the draft
491 genome. To recruit the 16S rRNA gene, BLASTn was used to identify the contigs with
492 *Prosthecochloris*-related 16S rRNA genes with an identity of >97%. Only one
493 *Prosthecochloris*-related 16S rRNA gene was identified in each culture, consistent with the
494 finding that only one CAP genome was recovered. Based on these results, the each contig
495 containing *Prosthecochloris* 16S rRNA gene was moved into the CAP draft genomes.

496

497 **Average nucleotide identity (ANI) calculation and phylogenetic analysis**

498 The ANIs between genomes were determined using the ANI calculator (52) and the
499 ANI matrices were visualized using the pheatmap function (53) in R (R core team, 2016).
500 To analyze the 16S rRNA gene phylogeny of *Chlorobiaceae* and *Halodesulfovibrio*, the
501 available *Chlorobiaceae* genomes and representative *Desulfovibrio* genomes were
502 retrieved from the RefSeq database (August 2019) (54) and 16S rRNA gene sequences in
503 the genomes were extracted by Barrnap v0.9 (55). On the other hand, *Halodesulfovibrio*
504 16S rRNA gene sequences were downloaded from the NCBI 16S rRNA database and

505 included in the analysis. A multiple sequence alignment of these 16S rRNA genes was
506 performed using MUSCLE (56), followed by a tree reconstruction by the Maximum
507 Likelihood method based on the Jukes-Cantor model and initial tree generation using the
508 BioNJ method in MEGA7 (57, 58). The confidence levels of the tree were determined using
509 1000 bootstraps (59).

510 For the FMO phylogeny, the FMO proteins were retrieved from the available
511 *Chlorobiaceae* genomes in RefSeq database (54). A tree was then inferred using the
512 Maximum Likelihood method based on the JTT matrix-based model (60) and initial tree
513 generation using the BioNJ method in MEGA7 (57) with 1000 bootstraps.

514 A tree was built from single-copy marker genes using the ezTree pipeline (61). Briefly,
515 the putative genes in the genomes were identified by Prodigal (62), and the Pfam profiles
516 of these genes were annotated using HMMER3 (63). Gene annotations were compared to
517 identify single-copy marker genes among the input genomes. The amino acid sequences of
518 single-copy marker genes were then aligned by MUSCLE (56). The alignments were
519 trimmed using Gblocks (64), and a tree based on the concatenated alignment was
520 constructed by Maximum Likelihood using FastTree with 1000 bootstraps (59, 65).

521

522 **Pan-genome analysis**

Bacterial Pan Genome Analysis tool (BPGA) v1.3 (66) was used to perform a pan-genome analysis. The genes in the *Prosthecochloris* genomes were first clustered using USEARCH (67) with a 70% identity cutoff. Gene clusters present in all the genome were defined as core genes, and those present in at least two—but not all—of the genomes were defined as accessory genes. The representative sequences of CAP-specific accessory genes were then searched against the NCBI RefSeq database (54) to identify the potential orthologous genes in bacteria, with 40% identity and 50% alignment length cutoffs. In addition, the dN/dS values of each CAP-unique accessory gene were determined using the HyPhy tool in MEGA7 (57).

Data Availability

Sequence reads of metagenomes have been submitted to NCBI sequence read archive (SRA) under SRA accession numbers SRR10714424, SRR10714423, SRR10714422, and SRR10714421, respectively. Supplementary data for this preprint is available on request to the corresponding author.

Acknowledgements

This study was supported by funding from Academia Sinica. Y.H.C would like to acknowledge the Taiwan International Graduate Program (TIGP) for its fellowship towards his graduate studies. We would like to thank Noah Last of Third Draft Editing for his

English language editing.

Author contribution

Y.H.C, S.H.Y, and S.L.T conceived the idea for this study. Y.H.C and S.H.Y assembled the genomes, performed the bioinformatics analysis, and wrote the manuscript. K.T helped write the manuscript and modify the illustrations. C.Y.L and H.J.C collected coral skeleton samples and prepared the DNA samples. C.J.S provided the cultures. S.L.T supervised the overall study. All authors read and approved the manuscript.

Conflict of Interest

The authors declare that they have no conflict of interest.

References

1. Rosenberg E, Koren O, Reshef L, Efrony R, Zilber-Rosenberg I. 2007. The role of microorganisms in coral health, disease and evolution. Nat Rev Microbiol 5:355-62.

2. Pollock FJ, McMinds R, Smith S, Bourne DG, Willis BL, Medina M, Thurber RV, Zaneveld JR. 2018. Coral-associated bacteria demonstrate phylosymbiosis and cophylogeny. Nat Commun 9:4921.

3. Dunphy CM, Gouhier TC, Chu ND, Vollmer SV. 2019. Structure and stability of the coral microbiome in space and time. Sci Rep 9:6785.

4. van Oppen MJH, Blackall LL. 2019. Coral microbiome dynamics, functions and

559 design in a changing world. Nat Rev Microbiol 17:557-567.

560 5. Gordon BR, Leggat W. 2010. Symbiodinium-Invertebrate Symbioses and the Role
561 of Metabolomics. Marine Drugs 8:2546-2568.

562 6. Lesser MP, Falcon LI, Rodriguez-Roman A, Enriquez S, Hoegh-Guldberg O, Iglesias-
563 Prieto R. 2007. Nitrogen fixation by symbiotic cyanobacteria provides a source of
564 nitrogen for the scleractinian coral Montastraea cavernosa. Marine Ecology
565 Progress Series 346:143-152.

566 7. Cai L, Zhou GW, Tian RM, Tong HY, Zhang WP, Sun J, Ding W, Wong YH, Xie JY, Qiu
567 JW, Liu S, Huang H, Qian PY. 2017. Metagenomic analysis reveals a green sulfur
568 bacterium as a potential coral symbiont. Scientific Reports 7.

569 8. Koren O, Rosenberg E. 2006. Bacteria associated with mucus and tissues of the
570 coral Oculina patagonica in summer and winter. Applied and Environmental
571 Microbiology 72:5254-5259.

572 9. Reis AMM, Araujo SD, Moura RL, Francini RB, Pappas G, Coelho AMA, Kruger RH,
573 Thompson FL. 2009. Bacterial diversity associated with the Brazilian endemic reef
574 coral Mussismilia braziliensis. Journal of Applied Microbiology 106:1378-1387.

575 10. Li ZY, Wang YZ, He LM, Zheng HJ. 2015. Metabolic profiles of prokaryotic and
576 eukaryotic communities in deep-sea sponge Neamphius huxleyi indicated by

577 metagenomics (vol 4, 3895, 2014). Scientific Reports 5.

578 11. Yang SH, Tandon K, Lu CY, Wada N, Shih CJ, Hsiao SSY, Jane WN, Lee TC, Yang CM,
579 Liu CT, Denis V, Wu YT, Wang LT, Huang LN, Lee DC, Wu YW, Yamashiro H, Tang SL.
580 2019. Metagenomic, phylogenetic, and functional characterization of
581 predominant endolithic green sulfur bacteria in the coral Isopora palifera.
582 Microbiome 7.

583 12. del Campo J, Pombert JF, Slapeta J, Larkum A, Keeling PJ. 2017. The 'other' coral
584 symbiont: Ostreobium diversity and distribution. Isme Journal 11:296-299.

585 13. Yang SH, Lee STM, Huang CR, Tseng CH, Chiang PW, Chen CP, Chen HJ, Tang SL.
586 2016. Prevalence of potential nitrogen-fixing, green sulfur bacteria in the skeleton
587 of reef-building coral Isopora palifera. Limnology and Oceanography 61:1078-1086.

588 14. Schlichter D, Kampmann H, Conrady S. 1997. Trophic potential and photoecology
589 of endolithic algae living within coral skeletons. Marine Ecology-Pubblicazioni Della
590 Stazione Zoologica Di Napoli I 18:299-317.

591 15. Fine M, Loya Y. 2002. Endolithic algae: an alternative source of photoassimilates
592 during coral bleaching. Proceedings of the Royal Society B-Biological Sciences
593 269:1205-1210.

594 16. Imhoff JF. 2014. Biology of Green Sulfur Bacteria. eLS John Wiley & Sons, Ltd:

595 Chichester.

596 17. Crowe SA, Hahn AS, Morgan-Lang C, Thompson KJ, Simister RL, Lliros M, Hirst M,
597 Hallam SJ. 2017. Draft Genome Sequence of the Pelagic Photoferrotroph
598 Chlorobium phaeoferrooxidans. Genome Announc 5.

599 18. Heising S, Richter L, Ludwig W, Schink B. 1999. Chlorobium ferrooxidans sp. nov., a
600 phototrophic green sulfur bacterium that oxidizes ferrous iron in coculture with a
601 "Geospirillum" sp. strain. Arch Microbiol 172:116-24.

602 19. Thiel V, Tank M, Bryant DA. 2018. Diversity of Chlorophototrophic Bacteria
603 Revealed in the Omics Era. Annu Rev Plant Biol 69:21-49.

604 20. Biebl H, Pfennig N. 1978. Growth Yields of Green Sulfur Bacteria in Mixed Cultures
605 with Sulfur and Sulfate Reducing Bacteria. Archives of Microbiology 117:9-16.

606 21. Pernice M, Raina JB, Radecker N, Cardenas A, Pogoreutz C, Voolstra CR. 2019.
607 Down to the bone: the role of overlooked endolithic microbiomes in reef coral
608 health. ISME J doi:10.1038/s41396-019-0548-z.

609 22. Richter M, Rossello-Mora R. 2009. Shifting the genomic gold standard for the
610 prokaryotic species definition. Proc Natl Acad Sci U S A 106:19126-31.

611 23. Bryantseva IA, Tarasov AL, Kostrikina NA, Gaisin VA, Grouzdev DS, Gorlenko VM.
612 2019. Prosthecochloris marina sp. nov., a new green sulfur bacterium from the

613 coastal zone of the South China Sea. Arch Microbiol doi:10.1007/s00203-019-
614 01707-y.
615 24. Kimes NE, Johnson WR, Torralba M, Nelson KE, Weil E, Morris PJ. 2013. The
616 Montastraea faveolata microbiome: ecological and temporal influences on a
617 Caribbean reef-building coral in decline. Environmental Microbiology 15:2082-
618 2094.
619 25. Mulligan C, Fischer M, Thomas GH. 2011. Tripartite ATP-independent periplasmic
620 (TRAP) transporters in bacteria and archaea. FEMS Microbiol Rev 35:68-86.
621 26. Montesinos E, Guerrero R, Abella C, Esteve I. 1983. Ecology and Physiology of the
622 Competition for Light Between Chlorobium limicola and Chlorobium
623 phaeobacteroides in Natural Habitats. Appl Environ Microbiol 46:1007-16.
624 27. Harada J, Mizoguchi T, Satoh S, Tsukatani Y, Yokono M, Noguchi M, Tanaka A,
625 Tamiaki H. 2013. Specific gene bciD for C7-methyl oxidation in bacteriochlorophyll
626 e biosynthesis of brown-colored green sulfur bacteria. PLoS One 8:e60026.
627 28. Ong RH, King AJ, Mullins BJ, Cooper TF, Caley MJ. 2012. Development and
628 validation of computational fluid dynamics models for prediction of heat transfer
629 and thermal microenvironments of corals. PLoS One 7:e37842.
630 29. Teran E, Mendez ER, Enriquez S, Iglesias-Prieto R. 2010. Multiple light scattering

631 and absorption in reef-building corals. Appl Opt 49:5032-42.

632 30. Brune DC. 1989. Sulfur oxidation by phototrophic bacteria. Biochim Biophys Acta

633 975:189-221.

634 31. Frigaard NU, Dahl C. 2009. Sulfur metabolism in phototrophic sulfur bacteria. Adv

635 Microb Physiol 54:103-200.

636 32. Meyer B, Imhoff JF, Kuever J. 2007. Molecular analysis of the distribution and

637 phylogeny of the soxB gene among sulfur-oxidizing bacteria - evolution of the Sox

638 sulfur oxidation enzyme system. Environ Microbiol 9:2957-77.

639 33. Gregersen LH, Bryant DA, Frigaard NU. 2011. Mechanisms and evolution of

640 oxidative sulfur metabolism in green sulfur bacteria. Front Microbiol 2:116.

641 34. Holkenbrink C, Barbas SO, Mellerup A, Otaki H, Frigaard NU. 2011. Sulfur globule

642 oxidation in green sulfur bacteria is dependent on the dissimilatory sulfite

643 reductase system. Microbiology-Sgm 157:1229-1239.

644 35. Eisen JA, Nelson KE, Paulsen IT, Heidelberg JF, Wu M, Dodson RJ, Deboy R, Gwinn

645 ML, Nelson WC, Haft DH, Hickey EK, Peterson JD, Durkin AS, Kolonay JL, Yang F, Holt

646 I, Umayam LA, Mason T, Brenner M, Shea TP, Parksey D, Nierman WC, Feldblyum

647 TV, Hansen CL, Craven MB, Radune D, Vamathevan J, Khouri H, White O, Gruber

648 TM, Ketchum KA, Venter JC, Tettelin H, Bryant DA, Fraser CM. 2002. The complete

649 genome sequence of Chlorobium tepidum TLS, a photosynthetic, anaerobic,
650 green-sulfur bacterium. Proc Natl Acad Sci U S A 99:9509-14.
651 36. Takii S, Hanada S, Hase Y, Tamaki H, Uyeno Y, Sekiguchi Y, Matsuura K. 2008.
652 Desulfovibrio marinisediminis sp. nov., a novel sulfate-reducing bacterium isolated
653 from coastal marine sediment via enrichment with Casamino acids. Int J Syst Evol
654 Microbiol 58:2433-8.
655 37. Finster KW, Kjeldsen KU. 2010. Desulfovibrio oceani subsp. oceani sp. nov., subsp.
656 nov. and Desulfovibrio oceani subsp. galateae subsp. nov., novel sulfate-reducing
657 bacteria isolated from the oxygen minimum zone off the coast of Peru. Antonie
658 Van Leeuwenhoek 97:221-9.
659 38. Shivani Y, Subhash Y, Sasikala C, Ramana CV. 2017. Halodesulfovibrio
660 spirochaetisodalis gen. nov. sp. nov. and reclassification of four Desulfovibrio spp.
661 Int J Syst Evol Microbiol 67:87-93.
662 39. Riederer-Henderson MA, Wilson PW. 1970. Nitrogen fixation by sulphate-reducing
663 bacteria. J Gen Microbiol 61:27-31.
664 40. Zyakun AM, Lunina ON, Prusakova TS, Pimenov NV, Ivanov MV. 2009. Fractionation
665 of stable carbon isotopes by photoautotrophically growing anoxygenic purple and
666 green sulfur bacteria. Microbiology 78:757-768.

667 41. S. A. 2010. FastQC: a quality control tool for high throughput sequence data.
668 http://www.bioinformatics.babraham.ac.uk/projects/fastqc.
669 42. Bolger AM, Lohse M, Usadel B. 2014. Trimmomatic: a flexible trimmer for Illumina
670 sequence data. Bioinformatics 30:2114-20.
671 43. Li D, Liu CM, Luo R, Sadakane K, Lam TW. 2015. MEGAHIT: an ultra-fast single-node
672 solution for large and complex metagenomics assembly via succinct de Bruijn
673 graph. Bioinformatics 31:1674-6.
674 44. Kang DD, Froula J, Egan R, Wang Z. 2015. MetaBAT, an efficient tool for accurately
675 reconstructing single genomes from complex microbial communities. PeerJ
676 3:e1165.
677 45. Parks DH, Imelfort M, Skennerton CT, Hugenholtz P, Tyson GW. 2015. CheckM:
678 assessing the quality of microbial genomes recovered from isolates, single cells,
679 and metagenomes. Genome Res 25:1043-55.
680 46. Parks DH, Chuvochina M, Waite DW, Rinke C, Skarshewski A, Chaumeil PA,
681 Hugenholtz P. 2018. A standardized bacterial taxonomy based on genome
682 phylogeny substantially revises the tree of life. Nat Biotechnol 36:996-1004.
683 47. Langmead B, Salzberg SL. 2012. Fast gapped-read alignment with Bowtie 2. Nat
684 Methods 9:357-9.

685 48. Seemann T. 2014. Prokka: rapid prokaryotic genome annotation. Bioinformatics
686 30:2068-9.
687 49. Kanehisa M, Sato Y, Morishima K. 2016. BlastKOALA and GhostKOALA: KEGG Tools
688 for Functional Characterization of Genome and Metagenome Sequences. J Mol
689 Biol 428:726-731.
690 50. Kanehisa M, Sato Y. 2019. KEGG Mapper for inferring cellular functions from
691 protein sequences. Protein Sci doi:10.1002/pro.3711.
692 51. Elbourne LD, Tetu SG, Hassan KA, Paulsen IT. 2017. TransportDB 2.0: a database for
693 exploring membrane transporters in sequenced genomes from all domains of life.
694 Nucleic Acids Res 45:D320-D324.
695 52. Rodriguez-R LM, Konstantinidis KT. 2016. The enveomics collection: a toolbox for
696 specialized analyses of microbial genomes and metagenomes. PeerJ Preprints.
697 53. Kolde R. 2019. pheatmap: Pretty Heatmaps. R package version 1012.
698 54. Pruitt KD, Tatusova T, Brown GR, Maglott DR. 2012. NCBI Reference Sequences
699 (RefSeq): current status, new features and genome annotation policy. Nucleic
700 Acids Res 40:D130-5.
701 55. Seemann T. barrnap 0.9 : rapid ribosomal RNA prediction
702 https://github.com/tseemann/barrnap.

703 56. Edgar RC. 2004. MUSCLE: multiple sequence alignment with high accuracy and
704 high throughput. Nucleic Acids Res 32:1792-7.
705 57. Kumar S, Stecher G, Tamura K. 2016. MEGA7: Molecular Evolutionary Genetics
706 Analysis Version 7.0 for Bigger Datasets. Mol Biol Evol 33:1870-4.
707 58. T.H. J, C.R. C. 1969. Evolution of protein molecules. Mammalian Protein
708 Metabolism:21-132.
709 59. Felsenstein J. 1985. Confidence Limits on Phylogenies: An Approach Using the
710 Bootstrap. Evolution 39:783-791.
711 60. Jones DT, Taylor WR, Thornton JM. 1992. The rapid generation of mutation data
712 matrices from protein sequences. Comput Appl Biosci 8:275-82.
713 61. Wu YW. 2018. ezTree: an automated pipeline for identifying phylogenetic marker
714 genes and inferring evolutionary relationships among uncultivated prokaryotic
715 draft genomes. BMC Genomics 19:921.
716 62. Hyatt D, Chen GL, Locascio PF, Land ML, Larimer FW, Hauser LJ. 2010. Prodigal:
717 prokaryotic gene recognition and translation initiation site identification. BMC
718 Bioinformatics 11:119.
719 63. Eddy SR. 2011. Accelerated Profile HMM Searches. PLoS Comput Biol 7:e1002195.
720 64. Castresana J. 2000. Selection of conserved blocks from multiple alignments for

their use in phylogenetic analysis. Mol Biol Evol 17:540-52.

65. Price MN, Dehal PS, Arkin AP. 2010. FastTree 2--approximately maximum-likelihood trees for large alignments. PLoS One 5:e9490.

66. Chaudhari NM, Gupta VK, Dutta C. 2016. BPGA- an ultra-fast pan-genome analysis pipeline. Sci Rep 6:24373.

67. Edgar RC. 2010. Search and clustering orders of magnitude faster than BLAST. Bioinformatics 26:2460-2461.

Figure Legends

FIG 1. Molecular phylogenetic analysis of green sulfur bacteria. The phylogenetic trees of 16S rRNA (A), FMO protein (B), and protein sequences of concatenated single-copy genes (C) were constructed by the maximum-likelihood method with 1000 bootstraps. 27 green sulfur bacteria genomes in the RefSeq database and coral-associated GSB genomes were used to construct the tree. Other GSB included 12 *Chlorobium,* 1 *Pelodictyon,* and 4 *Chlorobaculum*. The genome and 16S rRNA sequences of *Fibrobacter succinogenes* S85 were used as the outgroup.

FIG 2. Putative syntrophic interaction between CAP and *Ca.* H. lyudaonia. Brown-colored *Ca*. P. isopraea dominated the lower section of the coral skeleton while green-colored *Ca*. P. sp. N1 dominated the upper lower section. The light intensity decreased with depth into the skeleton. The exchange of carbon, sulfur, and nitrogen compounds are denoted; important transports are indicated based on the genome annotation. The detailed model is described in the discussion.

Table 1. Qualities and putative taxon of each bins in metagenome from N1, N2, and N3 cultures.

Supplemental Materials

FIG S1. Heatmap of average nucleotide identity between two individual GSB genomes. Values of ANI < 70 are denoted as NA because values below 70% are not reliable.

FIG S2. Pan-genome analysis. (A) Core and Pan-Genome plot of *Prosthecochloris*. (B) Statistics from the pan-genome analysis, including number of core, unique, accessory, and exclusive absent genes.

FIG S3. COG (A) and KEGG (B) distributions of core, accessory, and unique genes from the pan-genome analysis.

FIG S4. Phylogenetic tree based on core genome. The protein sequences of 20 random orthologous gene clusters in the core genome were aligned by MUSCLE, and the tree were constructed and concatenated by the neighbor-joining method. The number of clade-specific accessory genes are shown in each branch.

FIG S5. Molecular phylogenetic analysis of green sulfur bacteria. (A) Phylogeny constructed from 16S rRNA from 20 *Desulfovibrio* genomes from the RefSeq database and

765 *Halodesulfovibrio* using the maximum-likelihood method with 1000 bootstraps. 28
766 sequences and 1562 position were involved in the analysis. Scare bar represents 0.02
767 changes per nucleotide site. (B) Similarity matrix between each of the two SRB genomes
768 created by Gegenees. The matrix was exported into a distance matrix, which was used to
769 generate a dendrogram by SplitsTree 4 with the neighbor joining method. The scare bar
770 indicates 1% difference among average BLASTN similarity scores.
771
772 **Table S1.** Mapped reads and inferred abundance of each bin in N1, N2, and N3
773 metagenomes.
774
775 **Table S2.** Genes present in CAP but absent in other *Chlorobi*.
776
777 **Table S3.** Metabolism pathways and ABC transporter in coral-associated *Prosthecochloris*.
778
779 **Table S4.** Metabolism pathways and transporter systems in *Halodesulfovibrio*.
780
781 **DATA SET S1.** Transporter genes annotated by transportDB 2.0 in coral-associated
782 *Prosthecochloris* and *Ca*. H. lyudaonia.

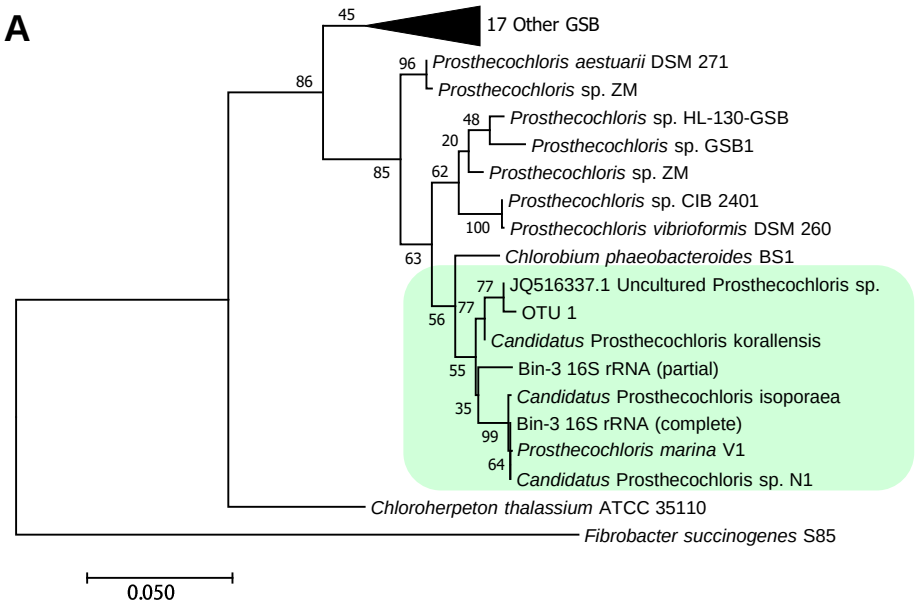

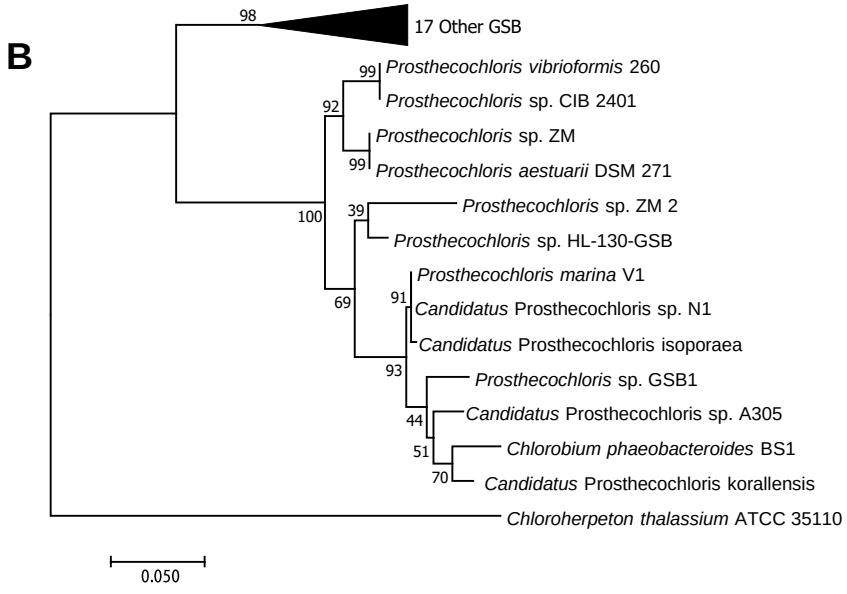

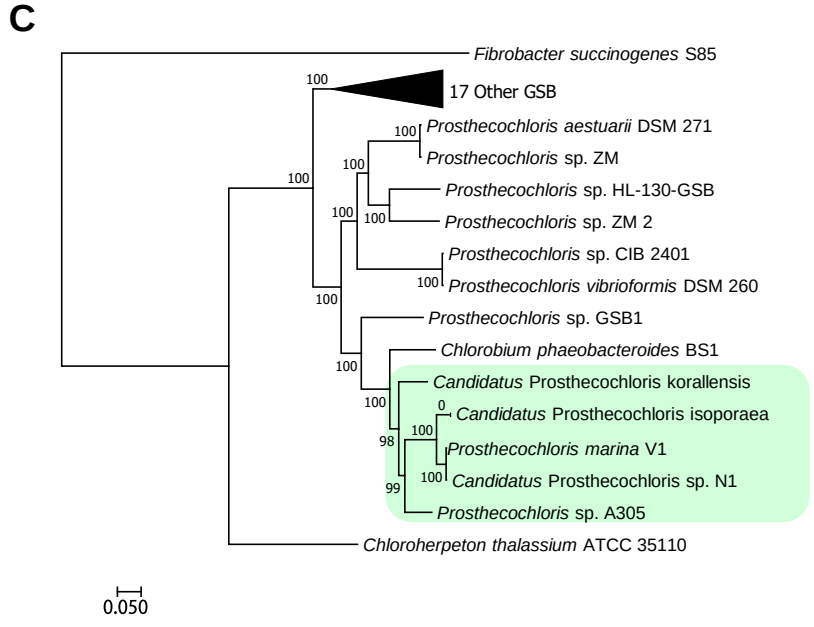

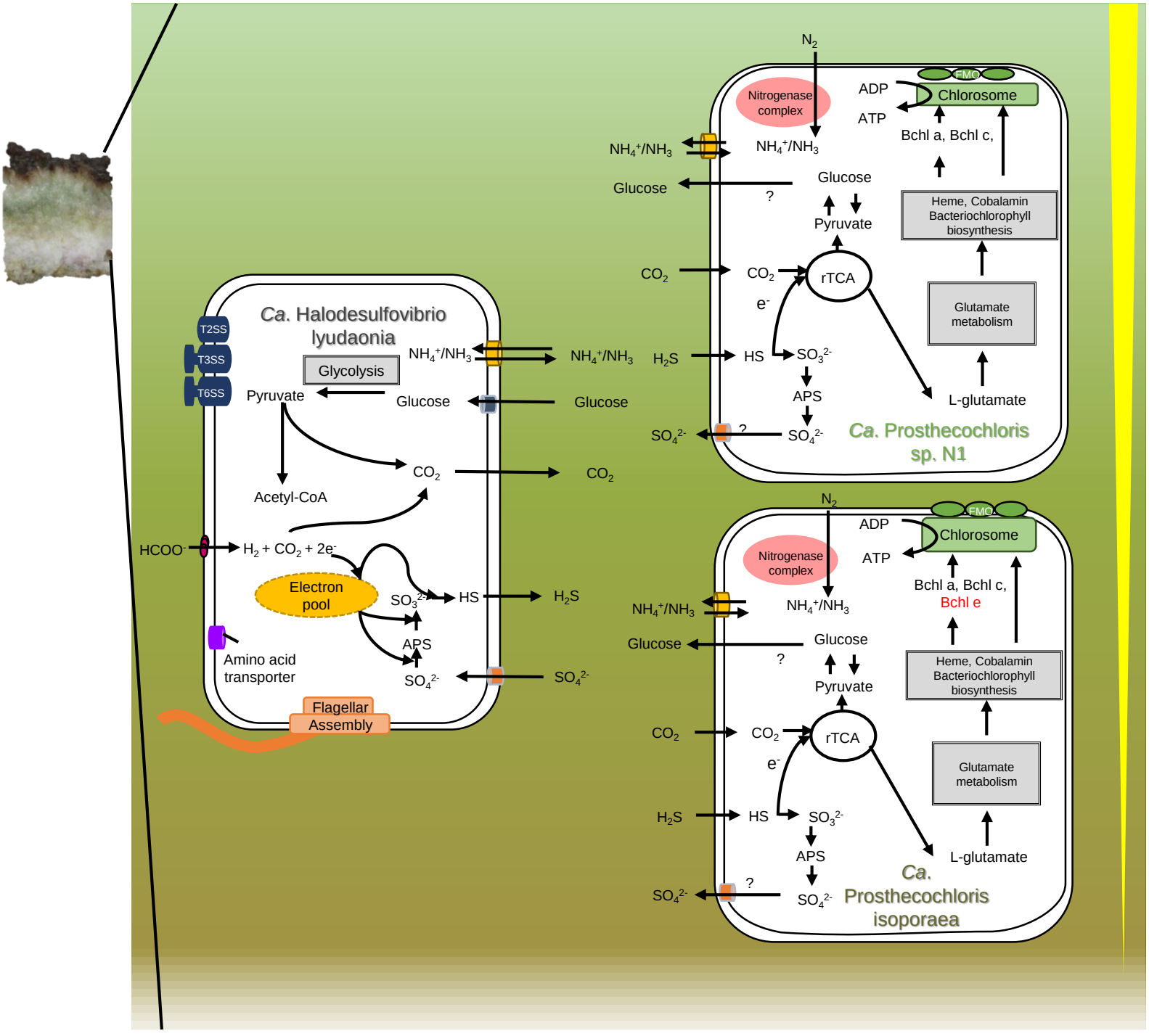

Table 1. Qualities and putative taxon of each bins in metagenome from N1, N2, and N3 cultures.

Bin Id	putative taxonomy	Completeness (%)	Contamation (%)	Strain heterogeneity	Genome size (bp)	# contigs	N50	Mean contig length (bp)	Longest contig (bp)	GC	# predicted genes
n1_1	*Marinifilum fragile*	99.46	2.15	0	4,632,452	67	126,188	69,141	306,114	35.7	3,843
n1_2	*Desulfuromonas* sp.	91.15	2.58	0	4,431,711	306	19,053	14,482	125,708	55.0	4,146
n1_3	*Halodesulfovibrio* sp.	100	0.56	33.33	4,215,690	43	163,138	98,039	320,254	45.1	3,684
n1_4	*Ilyobacter* sp.	94.38	1.12	0	2,867,017	124	32,721	23,121	160,652	36.3	2,715
n1_5	*Prosthecochloris marina*	99.43	1.37	0	2,785,587	24	205,628	116,066	495,280	47.0	2,648
n2_1	*Halodesulfovibrio* sp.	97.93	2.73	86.67	3,681,226	182	29,684	20,226	89,738	45.1	3,294
n2_2	*Desulfuromonas* sp.	63.38	2.58	40	2,938,736	622	4,902	4,724	22,680	55.8	3,037
n2_3	*Ilyobacter* sp.	96.63	1.12	0	2,896,854	127	33,041	22,809	160,613	36.3	2,742
n2_4	*Prosthecochloris* sp.	99.45	0.82	0	2,627,088	52	65,875	51,404	309,532	47.4	2,545
n2_5	*Desulfovibrio bizertensis*	80.85	1.18	0	2,284,992	440	5,709	5,193	28,696	52.6	2,379
n3_1	*Marinifilum* sp.	99.19	2.42	0	5,498,267	61	142,436	90,135	543,023	35.9	4,546
n3_2	*Pseudovibrio* sp.	85.04	0.79	0	5,165,768	718	8,788	7,194	35,672	50.0	5,091
n3_3	*Halodesulfovibrio* sp.	99.41	0.26	0	3,714,212	81	77,081	45,854	159,330	44.9	3,295
n3_4	*Prosthecochloris* sp.	98.90	0.82	0	2,630,645	50	79,255	52,612	225,631	47.4	2,545